Polyhedron 264 (2024) 117262

Contents lists available at ScienceDirect

Polyhedron

journal homepage: www.elsevier.com/locate/poly

Chiral and racemic BINOL spiroborate anions and radical-cation salt with BEDT-TTF

Joseph O. Ogar, Toby J. Blundell, Rifna Usman, Marek Vavrovič, Lee Martin *

School of Science and Technology, Nottingham Trent University, Clifton Lane, Clifton, Nottingham NG11 8NS, UK

ARTICLE INFO

Keywords:
Spiroborate
Boron
Chirality
BEDT-TTF
BINOL

ABSTRACT

Sodium salts of the spiroborate anion bis[(1,1′-*binaphthalene*)-2,2′-*diolato-O,O*′]borate in enantiopure and racemic forms have been obtained through reaction of BORAX (sodium tetraborate hexahydrate) with the corresponding stereoisomers of BINOL [(1,1′-binaphthalene)-2,2′-diol]. Electrocrystallisation of these salts with BEDT-TTF produces single crystals of a 1:1 radical-cation salt, (BEDT-TTF){B[1,1′-bis(BINOL)]$_2$}•THF, with the racemic spiroborate anion whilst no crystals were obtained with the enantiopure forms.

1. Introduction

Chirality in conducting materials has been of interest recently following the observations of electrical magneto-chiral anisotropy (eMChA) whereby the electrical resistance of the two enantiomers differs depending on their left- or right-handedness as well as on the direction of the electric current and applied magnetic field. eMChA has been observed in bismuth helices [1], carbon nanotubes [2,3], and trigonal tellurium [4], as well as in chiral magnets [5–7]. Field switchable chiral electrical transport has been demonstrated in achiral CsV_3Sb_5 [8]. Non-reciprocal charge transport has also been observed in non-centrosymmetric superconductors such as WS_2 nanotubes and MoS_2 thin single crystals [9,10].

Molecular materials with stereogenic centres can be synthesised in both enantiomeric forms and also as the racemate for comparison of their conducting properties. The first such bulk conductor to exhibit eMChA was (DM-EDT-TTF)$_2$ClO$_4$ a chiral metal down to 40 K, with the two enantiomers crystallising in enantiomorphic space groups $P6_222$ and $P6_422$ [11]. Chirality in these molecular radical-cation salts has been introduced through the use of chiral donor molecules [12], chiral anions [13,14], chiral guest molecules [15], or through chiral induction [16,17].

The utilisation of spiroborate anions in radical-cation salts can introduce multiple chiral centres into the material [18]. A tetrahedral boron centre with two achiral asymmetric bidentate ligands attached produces a spiroborate which is axially chiral at the boron centre (B_R and B_S). If the bidentate ligand has a stereogenic centre this will produce diastereomers of the spiroborate anion [18].

We have previously reported that chiral crystallisation may occur where only a specific enantiomer or diastereomer may enter the crystal despite using a racemic B(malate)$_2$ [18], B(mandelate)$_2$ [19], or B(2-chloromandelate)$_2$ [20] spiroborate anion as the starting material. One of these radical-cation salts, κ-BDH-TTP$_2$[B$_S$-(*S*-Cl-mandelate)$_2$], is metallic down to 4.2 K which is the lowest temperature for a chiral molecular metal [20]. Crystals of this type can have a macromolecular helical morphology when using chiral bidentate ligands on the spiroborate anion [19].

In this paper we present the synthesis of spiroborate anions from the axially chiral BINOL ligand [(1,1′-binaphthalene)-2,2′-diol] in the racemic, (*S*) and (*R*) forms and their subsequent electrocrystallisation with BEDT-TTF.

2. Experimental

2.1. Synthesis and purification of starting materials

(R)-(+)-1,1′-BINOL, (*S*)-(−)-1,1′-BINOL, 1,1′-BINOL, and bis(ethylenedithio)tetrathiafulvalene (BEDT-TTF) were purchased from TCI Chemicals. Ethanol, tetrahydrofuran, and dichloromethane were purchased from Fisher Scientific. 18-crown-6 was purchased from Sigma-Aldrich. All chemicals were used without further purification.

2.1.1. Synthesis of rac-1, (S,S)-1, (R,R)-1

BINOL (1.00 g, 3.5 mmol) in tetrahydrofuran (15 mL) was added to a

* Corresponding author.
E-mail address: lee.martin@ntu.ac.uk (L. Martin).

https://doi.org/10.1016/j.poly.2024.117262
Received 5 July 2024; Accepted 17 October 2024
Available online 22 October 2024

Table 1
Crystal data for ***rac*-1**, **(*R,R*)-1**, **(*S,S*)-1** and **2**.

Compound	*rac*-1	(*R,R*)-1	(*S,S*)-1	2
Empirical formula	$C_{48}H_{48}BNaO_8$	$C_{92}H_{84}B_2Na_2O_{14}$	$C_{92}H_{84}B_2Na_2O_{14}$	$C_{54}H_{40}BO_5S_8$
Formula weight	786.66	1481.19	1481.19	1036.15
Crystal system	Orthorhombic	Monoclinic	Monoclinic	Monoclinic
Space group	*Pbcn*	*C*2	*C*2	$P2_1/c$
a (Å)	18.7113(3)	25.9006(3)	25.8872(2)	17.4885(6)
b (Å)	10.5658(2)	8.25130(10)	8.25350(10)	16.2074(3)
c (Å)	20.4054(3)	17.8205(2)	17.83400(10)	18.2584(6)
α (°)	90	90	90	90
β (°)	90	101.8610(10)	101.9030(3)	117.240(4)
γ (°)	90	90	90	90
V (Å^3)	4034.14(12)	3727.17(8)	3728.48(6)	4601.3(3)
Z	4	2	2	4
Temperature/K	120.00(10)	143.00(30)	150.00(10)	120.00(12)
ρ_{calc} g/cm^3	1.295	1.320	1.319	1.496
μ/mm^{-1}	0.789	0.802	0.802	4.016
Reflection collected	31,528	108,598	36,354	60,220
Independent reflections	4038	7693	7320	9438
Flack parameter	–	−0.01(3)	0.03(2)	–
Final R indexes [I>=2σ (I)]	$R_1 = 0.0367$, $wR_2 = 0.1033$	$R_1 = 0.0439$, $wR_2 = 0.1238$	R1 = 0.0396, w*R*2 = 0.1103	$R_1 = 0.0392$, $wR_2 = 0.1076$
Final R indexes [all data]	$R_1 = 0.0388$, $wR_2 = 0.1051$	$R_1 = 0.0445$, $wR_2 = 0.1246$	$R_1 = 0.0404$, $wR_2 = 0.1120$	$R_1 = 0.0438$, $wR_2 = 0.1108$

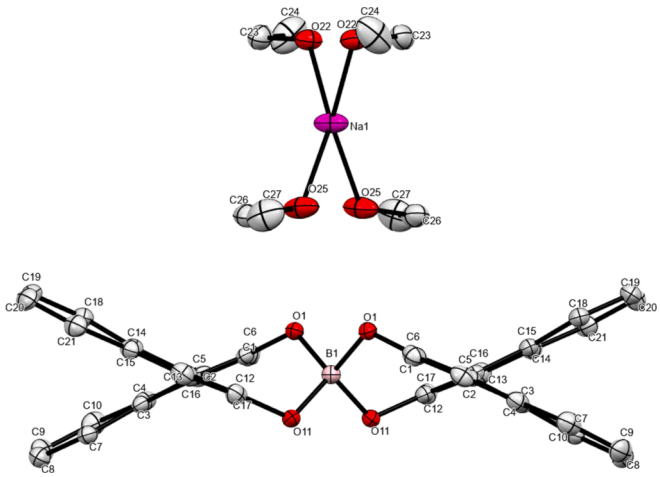

Fig. 1. ORTEP diagram of ***rac*-1** showing atomic labelling (H atoms have been omitted for clarity).

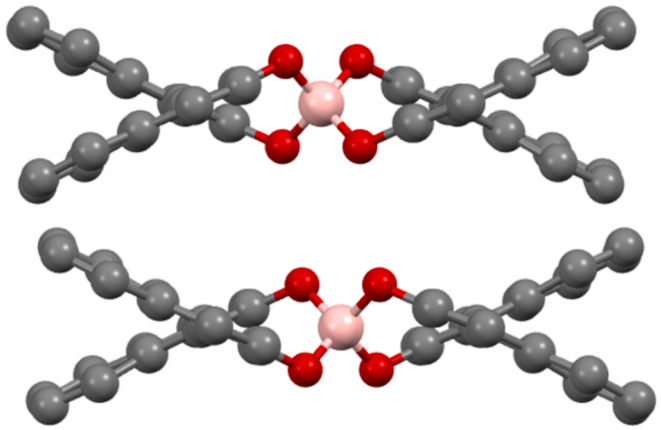

Fig. 2. The two enantiomers present in ***rac*-1**.

stirred solution of BORAX (180 mg, 0.46 mmol) and sodium hydroxide (40 mg, 1 mmol) in water (4 mL). The mixture was stirred at room temperature for 16 h and the solvents removed *in vacuo*. The white powder was recrystallised from ethanol to give clear cubic crystals. This method was previously reported by Carter *et al.* [21] to give a precipitate, however the three sodium salts ***rac*-1, (*S,S*)-1, (*R,R*)-1** have been obtained as single crystals with included ethanol molecules after recrystallisation.

***rac*-1:** IR (neat) 3644, 3054, 1587, 1504, 1465, 1427, 1364, 1242, 1070, 993, 953, 907, 813, 746 cm^{-1}; ^{1}H NMR (400 MHz, DMSO-D$_6$) *δ* 7.97 (d, *J* = 9.1 Hz, 4H), 7.94 (d, 4H), 7.33 (d, *J* = 8.7 Hz, 4H), 7.31 – 7.26 (m, 4H), 7.22 – 7.09 (m, 8H), 4.36 (s, 4H), 3.44 (qd, *J* = 7.0, 0.7 Hz, 8H), 1.06 (td, *J* = 7.0, 0.7 Hz, 12H); ^{13}C NMR (101 MHz, DMSO-*D*$_6$) *δ* 156.15, 132.86, 129.00, 128.26, 128.12, 125.87, 124.90, 124.60, 122.47, 121.89, 56.08, 18.61.

(*S,S*)-1: IR (neat) 3376, 3050, 2958, 2885, 1588, 1502, 1456, 1326, 1235, 987, 947, 898, 815, 742 cm^{-1}; ^{1}H NMR (400 MHz, DMSO-*D*$_6$) *δ* 7.97 (d, *J* = 8.7 Hz, 8H), 7.94 (d, *J* = 1.0 Hz, 8H), 7.34 (d, *J* = 8.7 Hz, 8H), 7.32 – 7.26 (m, 8H), 7.21 – 7.10 (m, 16H), 4.39 (s, 6H), 3.45 (q, *J* = 7.0 Hz, 12H), 1.06 (t, *J* = 7.0 Hz, 18H); ^{13}C NMR (101 MHz, DMSO-*D*$_6$) *δ* 156.16, 132.86, 129.00, 128.26, 128.12, 125.87, 124.90, 124.60, 122.48, 121.89, 56.08, 18.61.

(*R,R*)-1: IR (neat) 3380, 3052, 2970, 2886, 1589, 1502, 1460, 1364, 1327, 1236, 990, 948, 898, 813, 740; ^{1}H NMR (400 MHz, DMSO-*D*$_6$) *δ* 7.98 (d, *J* = 8.8 Hz, 8H), 7.94 (d, *J* = 1.1 Hz, 8H), 7.34 (d, *J* = 8.7 Hz, 8H), 7.32 – 7.25 (m, 8H), 7.21 – 7.10 (m, 16H), 4.38 (s, 6H), 3.45 (q, *J* = 7.0 Hz, 11*H*), 1.06 (t, *J* = 7.0 Hz, 15H); ^{13}C NMR (101 MHz, DMSO-*D*$_6$) *δ* 156.15, 132.85, 128.99, 128.24, 128.10, 125.86, 124.87, 124.59, 122.45, 121.88, 56.07, 18.60.

Note: The ^{1}H NMR peak (s) around *δ* 3.37 in all the spectra is attributed to water as an impurity. NMR spectra were measured in DMSO-*D*$_6$ owing to poor solubility in $CDCl_3$.

2.1.2. Synthesis of (BEDT-TTF){B[(1,1′-binaphthalene)-2,2′-diolato-O,O′]$_2$}•THF (2)

Single crystals were grown on platinum electrodes *via* electrocrystallisation in H-shaped cells in the dark on a vibration-free bench. The electrodes were cleaned by applying a voltage across the electrodes in 1 M H_2SO_4 in each direction to produce H_2 and O_2 at the electrodes, then washing with distilled water, methanol, and thoroughly dried. 100 mg of Na(EtOH)$_4$][B(1,1′-bis(BINOL)]$_2$ (***rac*-1**) and 200 mg 18-crown-6 was dissolved in tetrahydrofuran 26 mL:dichloromethane 13 mL with

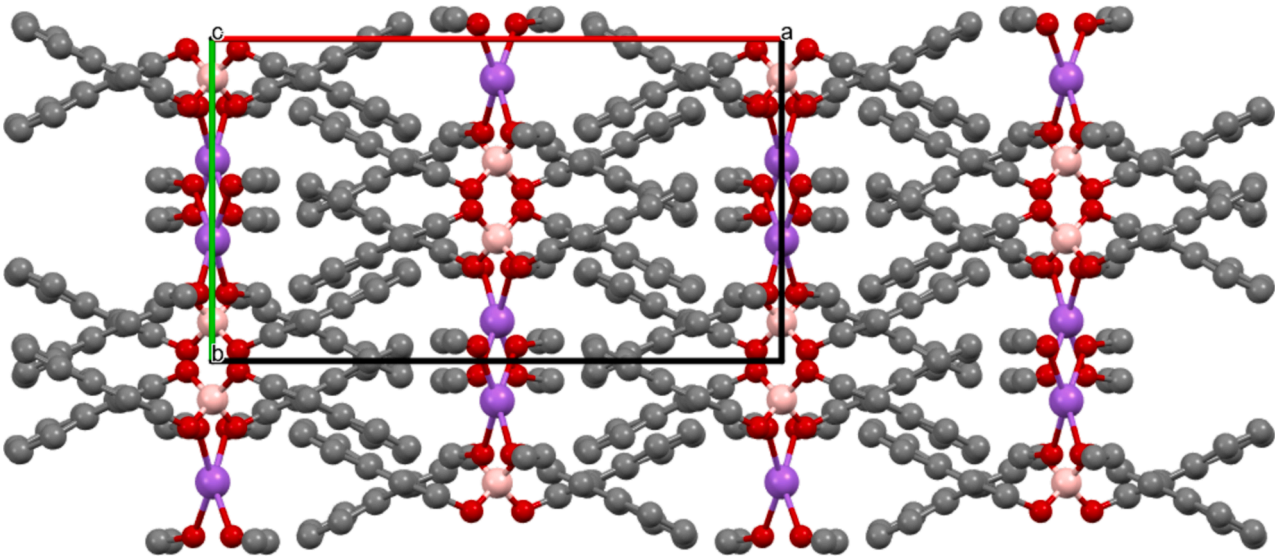

Fig. 3. ***Rac*-1** viewed down the *c* axis showing alternating enantiomers in stacks in the *b* direction.

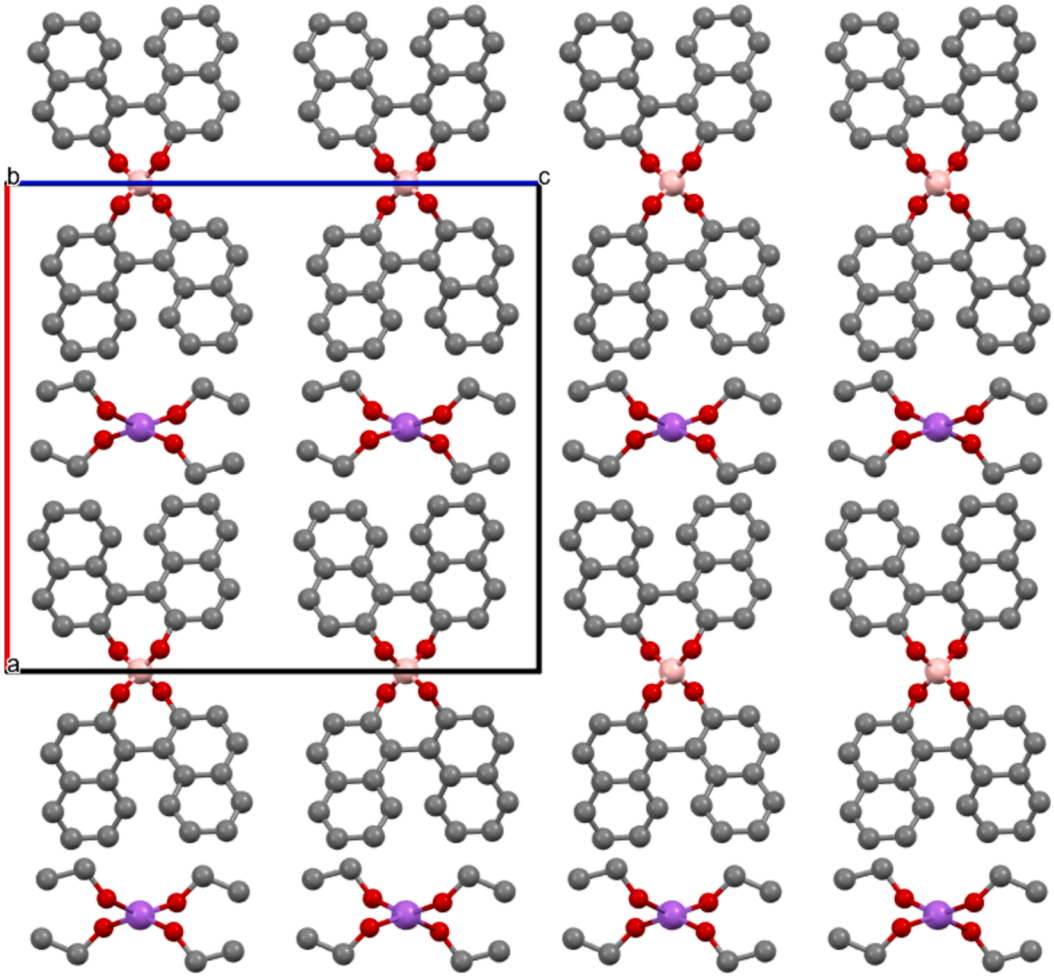

Fig. 4. ***Rac*-1** viewed down the *b* axis showing alternating enantiomers in stacks in the *c* direction.

stirring overnight. The solution was poured into a H-shaped cell containing 10 mg BEDT-TTF in the anode side and the cell was sonicated for 5 min. A constant current of 0.6 μA was applied for 11 days followed by 1.0 μA for a further 17 days, after which black crystals were collected from the electrode.

No crystals were obtained using this method with the enantiopure **(*S,S*)-1** or **(*R,R*)-1**. Further experiments using tetrahydrofuran, dichloromethane, chlorobenzene, or acetophenone also gave no crystals.

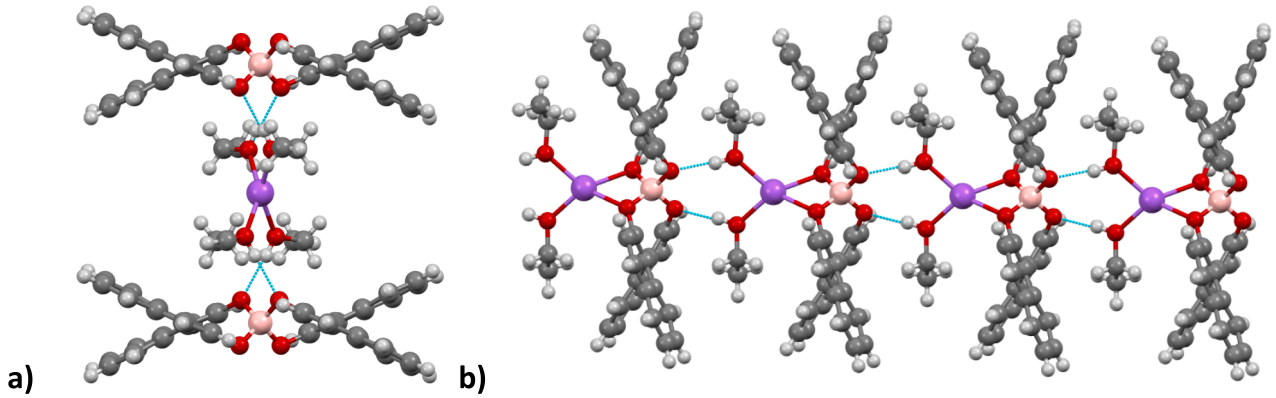

Fig. 5. Hydrogen bonding (shown using broken cyan lines) in (a) ***rac*-1** and (b) **(*S,S*)-1B.** ((Colour online.))

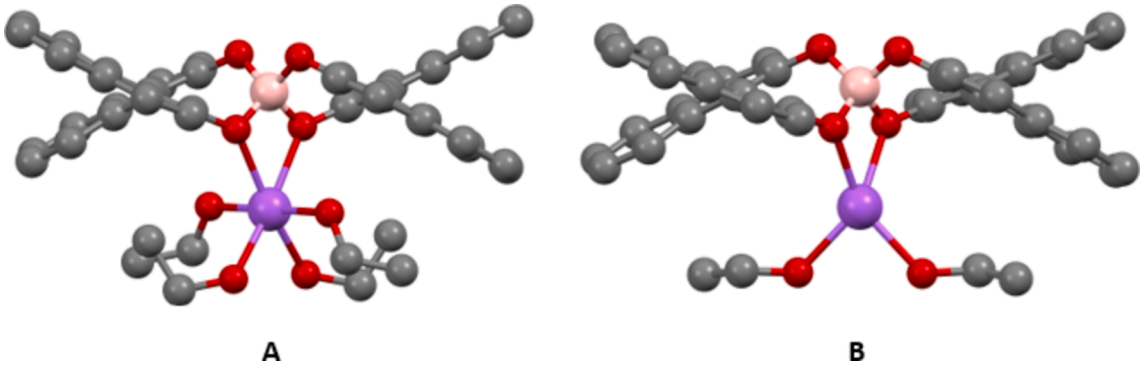

Fig. 6. The two crystallographically independent $B(BINOL)_2$ molecules in **(*R,R*)-1**, one having a sodium with 4 coordinated ethanol molecules (**A** – left) and the other having a sodium with 2 coordinated ethanol molecules (**B**- right).

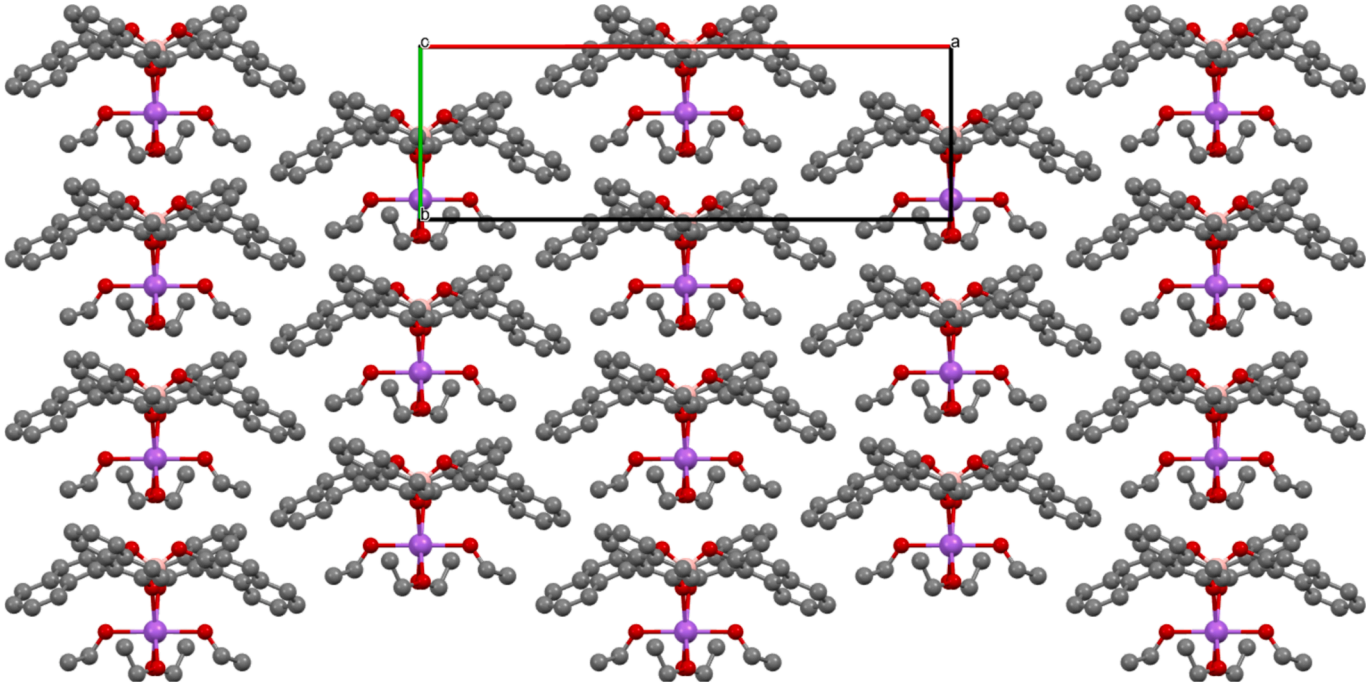

Fig. 7. A layer of the crystallographically independent $B(BINOL)_2$ molecule **A** in **(*R,R*)-1** having a sodium with 4 coordinated ethanol molecules viewed down the *c* axis.

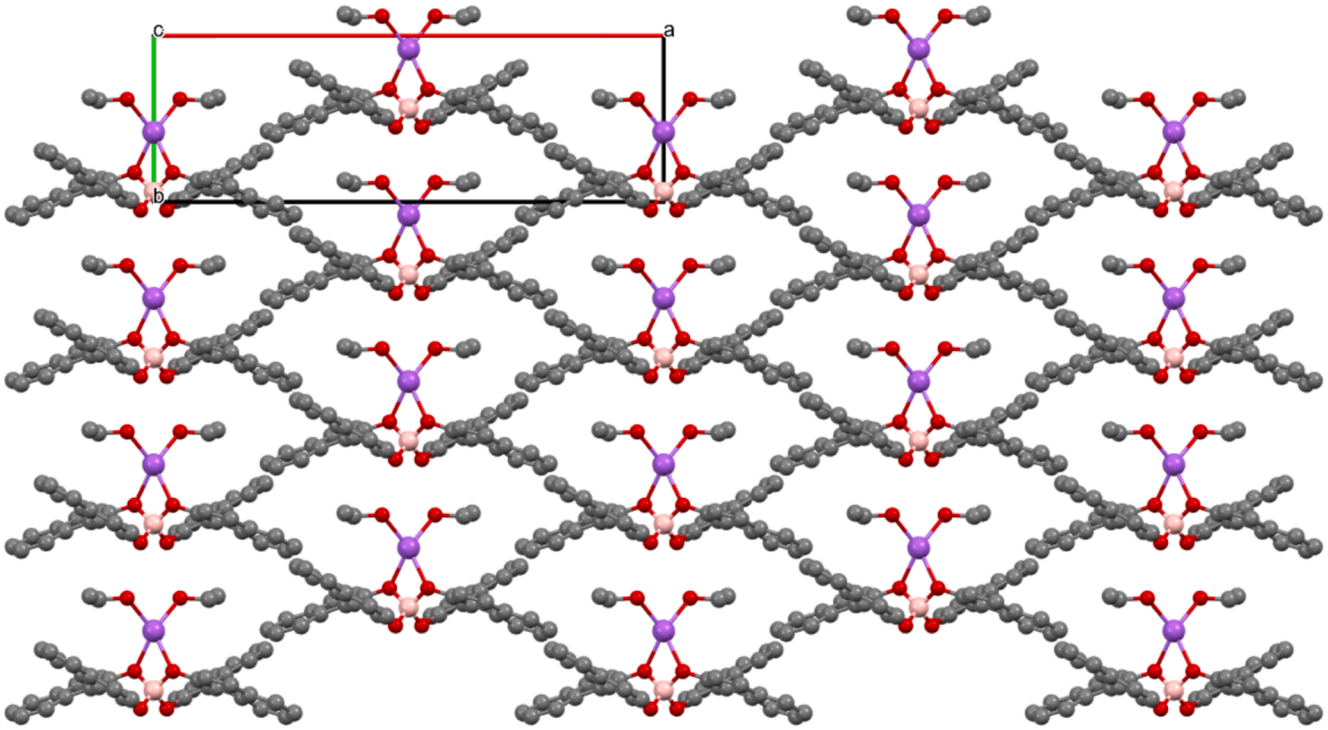

Fig. 8. A single layer of the crystallographically independent $B(BINOL)_2$ molecule **B** in ***(R,R)*-1** having a sodium with 2 coordinated ethanol molecules viewed down the *c* axis.

Table 2
Some important distances and angles. [A] and [B] represent the two crystallographically independent spiroborates related to the boron centres B1 and B2, respectively. [C]Data patterns to the spiroborate moiety in **2**. *The plane relates to each six-membered aromatic ring in each naphthyl unit.

	Rac-1	(*R*,*R*)-1[A]	(*S*,*S*)-1[A]	(*R*,*R*)-1[B]	(*S*,*S*)-1[B]	2[C]
Mean B-O bond length (Å)	1.468	1.467	1.468	1.468	1.467	1.468
O-B-O angles (°)	101.65, 102.22, 113.08, 113.65	101.40, 101.80, 112.59, 114.52	101.30, 101.80, 112.59, 114.55	99.70, 103.10, 112.25, 115.06	99.60, 102.80,112.32, 115.20	102.93 103.39 112.20 113.11 112.97 112.57
C—O—B-O Torsional angles (°)	42.22,43.67	42.50,42.80	42.70, 42.70	38.00, 47.40	38.10, 47.30	40.05 46.04 36.8648.69
*Benzyl to benzyl normal plane angles (°)	3.26,4.50	3.94,5.14	3.94, 4.98	2.37,3.56	2.37,3.64	3.05, 4.42, 4.79,5.98
Naphthyl to naphthyl normal plane angles (°)	51.08	54.93	55.01	51.46	51.48	53.1959.10

2.2. Single-crystal X-ray diffraction

Data (See Table1) for ***rac*-1**, **(*S*,*S*)-1**, **(*R*,*R*)-1**, and **2** were collected on a Rigaku Oxford Diffraction XtaLAB Synergy R, DW system, HyPix-Arc 100 using CuKα radiation using CrysAlis[Pro] software [22]. Using Olex-2 [23], the structures were solved with the SHELXT [24] structure solution program using Intrinsic Phasing and refined with the SHELXL [25] refinement package using Least Squares minimisation. All hydrogen atoms were placed in geometrically calculated positions; non-hydrogen atoms were refined with anisotropic displacement parameters. Molecular illustrations were prepared with Mercury [26].

3. Results and discussion

3.1. Structure discussion for rac-1

The ***rac*-1** salt crystallises in the orthorhombic space group *Pbcn*. The asymmetric unit contains half of a B[1,1′-bis(BINOL)]$_2$ anion and half of a sodium cation with two ethanol molecules coordinated to it. The boron and the sodium atoms both lie on a 2-fold axis, thus the salt has the formula: $[Na(EtOH)_4][B(1,1'\text{-bis(BINOL)}]_2$ with four of each species in the unit cell (Fig. 1). Thus, ***rac*-1** crystallises as a 1:1 mixture of the homochiral (*R*,*R*) and (*S*,*S*) enantiomers of B[1,1′-bis(BINOL)]$_2$ (Fig. 2). The anion has C_2 symmetry along three axes and a flattened disk-shaped D_2 conformation. A heterochiral (*R*,*S*) form is also possible, but our observed preference of the homochiral forms over the heterochiral has previously been seen with a variety of counter cations [27]. This is despite DFT calculations finding minimal thermodynamic difference between the homo- and heterochiral forms of the isolated anion [28]. The bulkiness of the *R*,*S* form has been attributed as a reason why the racemic form adopts the disk-shaped conformation in the (*R*,*R*) and (*S*,*S*) enantiopure forms [28].

Figs. 3 and 4 show the packing of the structure viewed down the *c* and *b* axes, respectively. The (*R*,*R*) and (*S*,*S*) diastereomers lie in

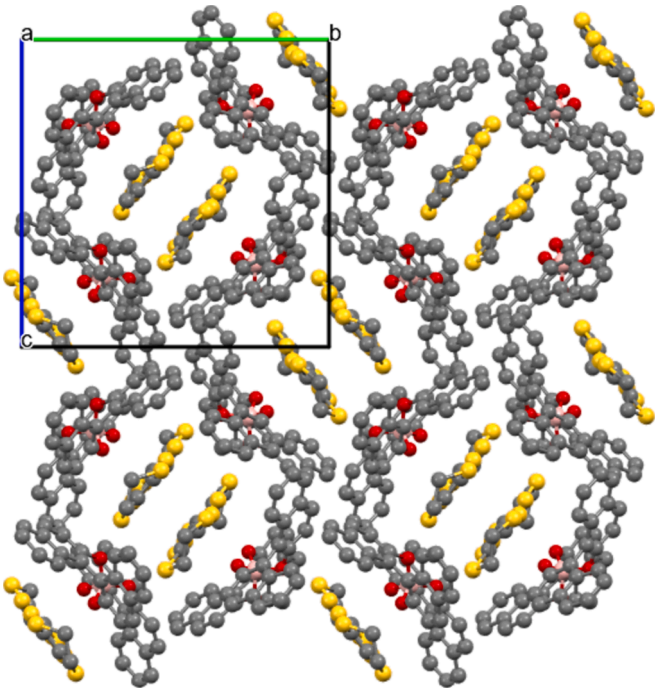

Fig. 9. The BEDT-TTF dimers each segregated by two *R,R*- and two *S,S*- B $(BINOL)_2$ molecules viewed down the *c* axis (solvent molecules have been occluded for clarity).

segregated rows with adjacent rows alternating between diastereomers in both the *b* and *c* directions. The sodium counterion is located between two moieties of the spiroborates with Na···B distance of 5.247 Å. The four ethanol molecules are coordinated to the cation such that hydrogen bonding (O1···H25 = 2.119 Å and O11···H22 = 2.090 Å) is possible as shown in Fig. 5(a). The four-coordinate sodium ion is far from tetrahedral, with two O-Na-O angles being 151.7°.

3.2. Structure discussion for (R,R)-1 and (S,S)-1

(*R,R*)-1 and **(*S,S*)-1** are isostructural crystallising in the non-centrosymmetric monoclinic space group *C*2. Crystallographic details are provided in Table 1. The asymmetric unit contains two half B[1,1′-bis(BINOL)]$_2$ units, two half sodium atoms, and three ethanol molecules. The salt has a formula of {Na[B(1,1′-bis(BINOL))$_2$(EtOH)$_4$]}{Na[B(1,1′-bis(BINOL))$_2$(EtOH)$_2$]}. The B[1,1′-bis(BINOL)]$_2$ anions are enantiopure having the same disk-shaped conformation and D_2 symmetry observed in the racemate – which is a 1:1 mixture of (*R,R*) and (*S,S*) (Fig. 2). In both of these enantiopure salts **(*R,R*)-1** and **(*S,S*)-1** the B[1,1′-bis(BINOL)]$_2$ anion adopts two different environments with one crystallographically independent anion having four ethanol molecules (**A** – Fig. 6 left) coordinated to its sodium cation which is six-coordinate including Na···O interactions with two BINOL oxygens. The other anion has only two ethanol molecules (**B** – Fig. 6 right) coordinated to its sodium cation which is four-coordinate, also including Na···O interactions with two BINOL oxygens. The B[1,1′-bis(BINOL)]$_2$ anions **A** and **B** stack in separate layers in the *c* direction as shown in Figs. 7 and 8. The coexistence of these two independent molecules is achieved through a synergistic ionic interaction between the $B(OC)_4$ units and the sodium counterions on the one hand and the hydrogen bonding between the ethanol OH hydrogen and the O of the $B(OC)_4$ units on the other hand (For **(*R,R*)-1:** O40···H51 = 1.965 Å, and for **(*S,S*)-1** O40···H51 = 1.968 Å). For instance, there exists hydrogen bonding (donor–acceptor (O52···O40) distance of 2.836(3) Å) which links the **(*S,S*)-1B** molecules together forming an infinite chain as shown in Fig. 5(b). Table 2 provides some useful bond lengths and angles for all the spiroborates reported in this study. For all the spiroborates the average B–O bond lengths for the central $B(OC)_4$ moiety is 1.4676 Å, consistent with those reported for similar borate salts [27,28]. The O–B–O bond angles range from 99.7(3) to 115.20(9) Å with the smallest and the largest bond angles found for the **(*S,S*)-1B**. As can be seen in Table 2, the structural features are similar for ***rac*-1**, **(*R,R*)-1A** and **(*S,S*)-1A** but markedly different for **(*R,R*)-1B** and **(*S,S*)-1B**. Both **(*R,R*)-1B** and **(*S,S*)-1B** have similar bond lengths and angles with more extreme torsional angles compared to those of ***rac*-1**, **(*R,R*)-1A** and **(*S,S*)-1A**.

In B[1,1′-bis(BINOL)]$_2$ crystals with amine cations the density of the enantiomerically pure crystals was lower than in the racemic ones. This was attributed to the chains of opposite enantiomers of the anion being able to pack more efficiently [28].[16] The opposite is true in the case of these sodium salts with coordinated ethanol molecules (Table 1).

3.3. Structure discussion for (BEDT-TTF){B[1,1′-bis(BINOL)]$_2$}·THF (2)

The spiroborate anions ***rac*-1, (*R,R*)-1** and **(*S,S*)-1** were each electrocrystallised with the donor molecule bis(ethylenedithio)tetrathiafulvalene (BEDT-TTF) using a variety of solvents. Crystals were only obtained in the combination of ***rac*-1** with tetrahydrofuran:dichloromethane. No crystals were obtained in the experiments with the enantiopure **(*R,R*)-1** and **(*S,S*)-1** spiroborates. The racemate offers the possibility of more packing arrangements of these bulky anions with BEDT-TTF and the radical-cation salt that is formed from ***rac*-1** has a 1:1 mixture of both the (*R,R*) and (*S,S*) forms and includes tetrahydrofuran guest molecules.

The asymmetric unit of **2** contains a B[1,1′-bis(BINOL)]$_2$, a BEDT-TTF molecule and a tetrahydrofuran molecule, crystallising in the monoclinic space group $P2_1/c$. The 1:1 radical-cation salt has a formula of (BEDT-TTF){B[1,1′-bis(BINOL)]$_2$}·THF. The BEDT-TTF molecules do not form conducting stacks and are isolated as dimers each surrounded by four B[1,1′-bis(BINOL)]$_2$, two (*R,R*) and two (*S,S*) diastereomers (Fig. 9). The angles and mean B-O bond length in **2** are similar to those of the other structures as could be seen in Table 2.

There are intermolecular S···S contacts shorter than the van der Waals distance (3.6 Å) between the two BEDT-TTFs of each dimer (S54···S59 3.4307(7), S51···S56 3.5353(7), and S47···S50 3.4596(7) Å). The isolated dimers have a closest S···S contact of 6.8164(7) Å (S54···S59) between neighbouring dimers, indicating that there is no conduction pathway through the lattice.

Applying the method of Guionneau *et al.* [29][17] the charge of the BEDT-TTF molecule is estimated to be 1.08^+, which is as expected for to balance the 1^- charge of the spiroborate anion in this 1:1 radical-cation salt.

4. Conclusions

The sodium salts of the spiroborate anion bis[(1,1′-*binaphthalene*)-2,2′-*diolato-O,O*′]borate in both enantiopure forms and in racemic form have been prepared and crystallographically characterised. The racemic spiroborate salt contained a 1:1 mixture of the *R,R* and *S,S* anion with no *meso R,S* present. Only the racemic spiroborate anion could be incorporated into a salt on electrocrystallisation with BEDT-TTF. To include one of the enantiopure anions in such a salt, the next step will be to electrocrystallise with an enantiopure organosulfur donor to obtain a salt with both species in enantiopure form. There are a wide variety of different sized and shaped bidentate ligands which could produce spiroborate anions *via* this method. These anions can be used in radical-cation salts to produce a variety of different donor packing motifs with different conducting behaviours. These salts have the potential to combine conductivity, or even superconductivity, with chirality in the same material which is the goal of this research.

CRediT authorship contribution statement

Joseph O. Ogar: Writing – review & editing, Writing – original draft, Visualization, Supervision, Methodology, Investigation, Data curation. **Toby J. Blundell:** Investigation. **Rifna Usman:** Investigation. **Marek Vavrovič:** Investigation. **Lee Martin:** Writing – review & editing, Writing – original draft, Visualization, Supervision, Project administration, Methodology, Investigation, Funding acquisition, Data curation, Conceptualization.

Declaration of competing interest

The authors declare that they have no known competing financial interests or personal relationships that could have appeared to influence the work reported in this paper.

Acknowledgements

LM, JOO and TJB would like to thank the Leverhulme Trust for financial support (RPG-2019-242).

Appendix A. Supplementary data

CCDC contains the supplementary crystallographic data for CCDC-2341599 (**(*R,R*)-1**), CCDC-23415600 (***rac*-1**), CCDC-23415601 (**(*S,S*)-1**), CCDC-23415602 (**2**). These data can be obtained free of charge via https://www.ccdc.cam.ac.uk/conts/retrieving.html, or from the Cambridge Crystallographic Data Centre, 12 Union Road, Cambridge CB2 1EZ, UK; fax: (+44) 1223–336-033; or deposit@ccdc.cam.ac.uk. Supplementary data to this article can be found online at https://doi.org/10.1016/j.poly.2024.117262.

Data availability

Data will be made available on request.

References

[1] G.L.J.A. Rikken, J. Fölling, P. Wyder, Electrical Magnetochiral Anisotropy, Phys. Rev. Lett. 87 (2001) 236602, https://doi.org/10.1103/PhysRevLett.87.236602.
[2] J. Wei, M. Shimogawa, Z. Wang, I. Radu, R. Dormaier, D.H. Cobden, Magnetic-Field Asymmetry of Nonlinear Transport in Carbon Nanotubes, Phys. Rev. Lett. 95 (2005) 256601, https://doi.org/10.1103/PhysRevLett.95.256601.
[3] V. Krstić, S. Roth, M. Burghard, K. Kern, G.L.J.A. Rikken, Magneto-chiral anisotropy in charge transport through single-walled carbon nanotubes, J. Chem. Phys. 117 (2002) 11315–11319, https://doi.org/10.1063/1.1523895.
[4] G.L.J.A. Rikken, N. Avarvari, Strong electrical magnetochiral anisotropy in tellurium, Phys. Rev. B 99 (2019) 245153, https://doi.org/10.1103/PhysRevB.99.245153.
[5] R. Aoki, Y. Kousaka, Y. Togawa, Anomalous Nonreciprocal Electrical Transport on Chiral Magnetic Order, Phys. Rev. Lett. 122 (2019) 057206, https://doi.org/10.1103/PhysRevLett.122.057206.
[6] T. Yokouchi, N. Kanazawa, A. Kikkawa, D. Morikawa, K. Shibata, T. Arima, Y. Taguchi, F. Kagawa, Y. Tokura, Electrical magnetochiral effect induced by chiral spin fluctuations, Nat. Commun. 8 (2017) 866, https://doi.org/10.1038/s41467-017-01094-2.
[7] H. Maurenbrecher, J. Mendil, G. Chatzipirpiridis, M. Mattmann, S. Pané, B. J. Nelson, P. Gambardella, Chiral anisotropic magnetoresistance of ferromagnetic helices, Appl. Phys. Lett. 112 (2018) 242401, https://doi.org/10.1063/1.5027660.
[8] C. Guo, C. Putzke, S. Konyzheva, X. Huang, M. Gutierrez-Amigo, I. Errea, D. Chen, M.G. Vergniory, C. Felser, M.H. Fischer, T. Neupert, P.J.W. Moll, Switchable chiral transport in charge-ordered kagome metal CsV3Sb5, Nature 611 (2022) 461–466, https://doi.org/10.1038/s41586-022-05127-9.
[9] R. Wakatsuki, Y. Saito, S. Hoshino, Y.M. Itahashi, T. Ideue, M. Ezawa, Y. Iwasa, N. Nagaosa, Nonreciprocal charge transport in noncentrosymmetric superconductors, Sci. Adv. 3 (2017) e1602390.
[10] F. Qin, W. Shi, T. Ideue, M. Yoshida, A. Zak, R. Tenne, T. Kikitsu, D. Inoue, D. Hashizume, Y. Iwasa, Superconductivity in a chiral nanotube, Nat. Commun. 8 (2017) 14465, https://doi.org/10.1038/ncomms14465.
[11] F. Pop, P. Auban-Senzier, E. Canadell, G.L.J.A. Rikken, N. Avarvari, Electrical magnetochiral anisotropy in a bulk chiral molecular conductor, Nat. Commun. 5 (2014) 3757, https://doi.org/10.1038/ncomms4757.
[12] J.I. Short, T.J. Blundell, S.J. Krivickas, S. Yang, J.D. Wallis, H. Akutsu, Y. Nakazawa, L. Martin, Chiral molecular conductor with an insulator–metal transition close to room temperature, Chem. Commun. 56 (2020) 9497–9500, https://doi.org/10.1039/D0CC04094K.
[13] M. Clemente-León, E. Coronado, C.J. Gómez-García, A. Soriano-Portillo, S. Constant, R. Frantz, J. Lacour, Unusual packing of ET molecules caused by π–π stacking interactions with TRISPHAT molecules in two [ET][TRISPHAT] salts (ET=bis(ethylenedithio)tetrathiafulvalene, TRISPHAT=(tris (tetrachlorobenzenediolato)phosphate(V))), Inorganica Chim. Acta 360 (2007) 955–960, https://doi.org/10.1016/j.ica.2006.07.025.
[14] E. Coronado, J.R. Galán-Mascarós, C.J. Gómez-García, A. Murcia-Martínez, E. Canadell, A Chiral Molecular Conductor: Synthesis, Structure, and Physical Properties of [ET]3[Sb2(l-tart)2]·CH3CN (ET = Bis(ethylendithio) tetrathiafulvalene; l-tart = (2R,3R)-(+)-Tartrate), Inorg. Chem. 43 (2004) 8072–8077, https://doi.org/10.1021/ic049257e.
[15] L. Martin, P. Day, H. Akutsu, J. Yamada, S. Nakatsuji, W. Clegg, R.W. Harrington, P.N. Horton, M.B. Hursthouse, P. McMillan, S. Firth, Metallic molecular crystals containing chiral or racemic guest molecules, CrystEngComm 9 (2007) 865–867, https://doi.org/10.1039/B709558A.
[16] L. Martin, H. Akutsu, P.N. Horton, M.B. Hursthouse, Chirality in charge-transfer salts of BEDT-TTF of tris(oxalato)chromate(III), CrystEngComm 17 (2015) 2783–2790, https://doi.org/10.1039/C5CE00121H.
[17] L. Martin, H. Akutsu, P.N. Horton, M.B. Hursthouse, R.W. Harrington, W. Clegg, Chiral Radical-Cation Salts of BEDT-TTF Containing a Single Enantiomer of Tris (oxalato)aluminate(III) and -chromate(III), Eur. J. Inorg. Chem. 2015 (2015) 1865–1870, https://doi.org/10.1002/ejic.201500092.
[18] J.R. Lopez, L. Martin, J.D. Wallis, H. Akutsu, Y. Nakazawa, J. Yamada, T. Kadoya, S.J. Coles, C. Wilson, Enantiopure and racemic radical-cation salts of B(malate)2− anions with BEDT-TTF, Dalton Trans. 45 (2016) 9285–9293, https://doi.org/10.1039/C6DT01038E.
[19] T.J. Blundell, J.R. Lopez, K. Sneade, J.D. Wallis, H. Akutsu, Y. Nakazawa, S. J. Coles, C. Wilson, L. Martin, Enantiopure and racemic radical-cation salts of B (mandelate)2- and B(2-chloromandelate)2- anions with BEDT-TTF, Dalton Trans. 51 (2022) 4843–4852, https://doi.org/10.1039/D2DT00024E.
[20] T.J. Blundell, M. Brannan, H. Nishimoto, T. Kadoya, J. Yamada, H. Akutsu, Y. Nakazawa, L. Martin, Chiral metal down to 4.2 K – a BDH-TTP radical-cation salt with spiroboronate anion B(2-chloromandelate)$_2^-$, Chem. Commun. 57 (2021) 5406–5409, https://doi.org/10.1039/D1CC01441B.
[21] C. Carter, S. Fletcher, A. Nelson, Towards phase-transfer catalysts with a chiral anion: inducing asymmetry in the reactions of cations, Tetrahedron Asymmetry 14 (2003) 1995–2004, https://doi.org/10.1016/S0957-4166(03)00367-7.
[22] Rigaku Oxford Diffraction, (2022), CrysAlisPro Software system, version 171.42.49, Rigaku Corporation, Wroclaw, Poland, (n.d.). https://rigaku.com/products/crystallography/x-ray-diffraction/crysalispro.
[23] O.V. Dolomanov, L.J. Bourhis, R.J. Gildea, J.A.K. Howard, H. Puschmann, OLEX2: a complete structure solution, refinement and analysis program, J. Appl. Crystallogr. 42 (2009) 339–341, https://doi.org/10.1107/S0021889808042726.
[24] G.M. Sheldrick, SHELXT – Integrated space-group and crystal-structure determination, Acta Crystallogr. Sect. Found. Adv. 71 (2015) 3–8, https://doi.org/10.1107/S2053273314026370.
[25] G.M. Sheldrick, Crystal structure refinement with *SHELXL*, Acta Crystallogr. Sect. C Struct. Chem. 71 (2015) 3–8, https://doi.org/10.1107/S2053229614024218.
[26] C.F. Macrae, P.R. Edgington, P. McCabe, E. Pidcock, G.P. Shields, R. Taylor, M. Towler, J. Van De Streek, *Mercury* : visualization and analysis of crystal structures, J. Appl. Crystallogr. 39 (2006) 453–457, https://doi.org/10.1107/S002188980600731X.
[27] T. Tu, T. Maris, J.D. Wuest, Crystal Structures of Spiroborates Derived from [1,1′-Binaphthalene]-2,2′-diol (BINOL), Cryst. Growth Des. 8 (2008) 1541–1546, https://doi.org/10.1021/cg7008013.
[28] J.A. Raskatov, J.M. Brown, A.L. Thompson, Chiral selection in the formation of borates from racemic binaphthols and related diols, CrystEngComm 13 (2011) 2923–2929, https://doi.org/10.1039/C0CE00709A.
[29] P. Guionneau, C.J. Kepert, G. Bravic, D. Chasseau, M.R. Truter, M. Kurmoo, P. Day, Determining the charge distribution in BEDT-TTF salts, Synth. Met. 86 (1997) 1973–1974, https://doi.org/10.1016/S0379-6779(97)80983-6.